Intelligent Sliding Mode Scheme for Regenerative Braking Control

Sulakshan Rajendran* Sarah Spurgeon Georgios Tsampardoukas*** Ric Hampson*****

*Electronic and Electrical Engineering Department, University College London, UK
(e-mail: uceeraj@ucl.ac.uk , s.spurgeon@ucl.ac.uk)
*** Jaguar Land Rover, W/1/26 Abbey Road, Whitley, Coventry, CV3 4LF, UK
(e-mail: gtsampar@jaguarlandrover.com, rhampso2@jaguarlandrover.com)

Abstract: Controller design for an Anti-Lock Braking System (ABS) of a Hybrid Electric Vehicle (HEV) or Electric Vehicle (EV) is a challenging task because of the trade-off between braking efficiency and energy recuperation efficiency. In hybrid vehicles, the brake torque demand is met by both the conventional friction braking system and an electric Regenerative Braking System (RBS). Hence, an effective ABS controller is required to achieve high braking efficiency without losing energy recuperation efficiency. This paper presents an Intelligent Sliding Mode Scheme (ISMS) to retain high energy recuperation efficiency as well as good braking efficiency of an EV with a unique braking configuration. The ISMS has a supervisory logic based motor torque limiter and slip controller. The slip controller is designed based on a two-wheeled model which has a hydraulic unit at the front producing frictional braking cooperating with a regenerative braking system with a brake-by-wire unit at the rear wheels. The slip controller is designed considering the hydraulics and motor actuator dynamics and the complete Magic Formula (MF) is used for tyre force estimation. The logic-based torque limiter not only regulates the brake torque to follow an assigned brake force distribution but also ensures that the battery is not overcharged.

Keywords: SMC, ABS control, Vehicle Control, Nonlinear Control.

1. INTRODUCTION

The use of regenerative braking systems in EV or HEV vehicles for conventional frictional braking with a hydraulic unit to further reduce energy consumption is of significant interest to the automotive industry. Furthermore, increasing concern over CO_2 emissions is another major factor which has increased interest in regenerative braking systems across world leading automotive companies. Though EVs are widely considered for urban use in order maintain a low level of CO_2 emissions, the current battery capacity limits their effective functional range. Specifically, they fail to meet higher demands of braking force when only equipped with electric motors to generate that brake force. Hence, a thermal braking system or conventional braking system is usually operated with a RBS.

Most modern wheeled vehicles are equipped with ABS to prevent the wheels from locking during braking. During braking, the applied brake torque causes the wheels to slow down resulting in a deviation between the vehicle velocity and the wheel angular velocity. Hence, the vehicle starts to skid. The resulting so-called wheel-slip varies from a minimum of zero to a maximum of one. Zero slip implies that the linearised wheel velocity is the same as the vehicle speed and a slip of one suggests that the linearised wheel velocity is zero and the wheel is locked but the car is still moving, which corresponds to the vehicle skidding. The ABS not only prevents the wheels from locking but also produces high braking efficiency. This is achieved by maintaining the slip at an optimal value hence generating maximum frictional force. The tyre/road model is an important factor which determines the accuracy of the complex dynamics of the tyre-road interaction and hence, the performance of the controller. Moreover, the controller should be robust to any other external disturbances and uncertainties.

These requirements have motivated the use of sliding mode control methods for the ABS control problem, see for example the work of Wu et al (2001), Song et al (2005), Hamzah et al (2007), Oniz et al (2009) and Guo et al (2014). SMC exhibits high robustness to uncertainties and disturbances which renders it appropriate to fulfil the design requirements. Much of the literature, however, focuses on conventional ABS control with friction braking or the case of a fully electric vehicle. Moreover, the majority of authors focus on tracking a constant slip value without considering continuous variation in slip or do not consider simulation testing with high fidelity models. Particularly simple tyre-road models are frequently used to describe the tyre-road interaction.

In addition to the challenges involved in designing an efficient ABS controller, an effective brake force distribution scheme is required in an HEV to ensure high energy recuperation. If the brake force distribution is not managed effectively then the controller may fail to produce the required braking torque. Furthermore, the battery pack may incur damage due to overcharging caused by uncontrolled recuperation.

Oniz et al (2009) presented an ABS controller based on SMC with a grey-predictor to estimate the vehicle velocity and the wheel angular velocity. The proposed controller was tested with a two-wheel ABS prototype experimental setup and a quarter car model. Overall, it performed better than conventional approaches. An SMC controller based on an integral sliding surface design for an HEV is presented by Song et al (2005). Park et al (2006) designed an ABS controller based on SMC for an EV with Electro Mechanical Brakes (EMB) only. Jianjun at al (2017) discussed regenerative braking control strategies for an EV with Continuously Variable Transmission (CVT). Jing et al (2009) designed an SMC controller which included estimation of the frictional coefficient based on Artificial Neural Networks (ANN). A notable contribution on Fuzzy SMC (FSMC) presented by Guo et al (2014) considered an HEV with both hydraulic brakes and EMB. It produced good results with simulation tests but only a simple tyre-road model is used to describe the tyre-road interaction. There are numerous contributions which consider FSMC for HEV, see for example the work of Tur et al (2007) and Bera et al (2011), but the processing time required for practical implementation is not considered. This paper presents a simple logic based intelligent SM scheme for regenerative braking control where the processing time is considered a key design objective. Both actuator dynamics are considered within the design. The complete Magic formula (MF) is also used to describe the tyre-road dynamics and an Extended Kalman Filter (EKF) is used to update the shape coefficients of the model.

The paper is structured as follows. Section 2 presents the experimental vehicle and mathematical models: a 14th order full-car model is used for testing and a corresponding two-wheel model including both hydraulic and motor actuator systems is used for controller design. Section 3 presents a novel hybrid brake force distribution pattern incorporating the regenerative braking limitations. An optimal slip trajectory generator and a logic-based brake torque limiter are presented in Section 4. Section 5 presents a slip controller based on SMC considering actuator dynamics based on a two-wheel model and simulation test results. Concluding remarks and future work are addressed in Section 6.

2. VEHICLE MODEL

2.1 Experimental vehicle

The experimental vehicle used is a Delta E4 Coupe with two traction Electric Motors (EMs) that have been re-purposed to facilitate braking and slip control as shown in Fig.1. There are two identical electric motors at the rear axle and hydraulics at the front wheels. The vehicle is installed with wheel speed sensors, torques sensors and an Inertial Measurement Unit (IMU) to provide wheel speed, brake torque, acceleration and rotational rates respectively.

Fig.1. Delta E4 Coupe experimental vehicle

2.2 Nonlinear full -vehicle model

This is a 14th order model based on the prototype vehicle which is used to test the designed controllers before they are tested with the industrial simulation platform CarMaker prior to experimental testing. The heave, pitch and roll motions of the vehicle body are considered as described in Rajendran et al (2017). The state vector of the model is given as

$$x(t) = [v_x v_y \varphi \dot{\varphi} z_s \dot{z}_s \theta \dot{\theta} \phi \dot{\phi} F_x^{ij} F_y^{ij} \dot{F}_x^{ij} \dot{F}_y^{ij}]^T \quad (1)$$
$$u(t) = [T_b^{FL} T_b^{FR} T_b^{RL} T_b^{RR}]$$

where ij = *FL*, *FR*, *RL*, *RR* and the nomenclature identifies the front and rear (first superscript) and right and left (second superscript), respectively.

2.2 *Two-wheel model*

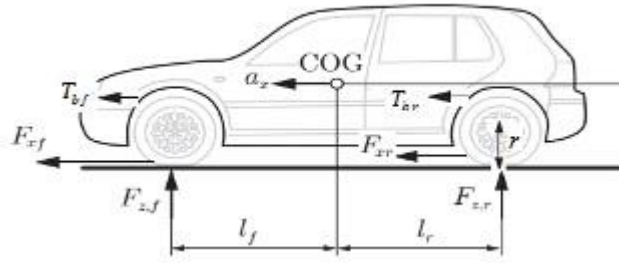

Fig.2. Two-wheel model

Fig.2 illustrates the free body diagram of a two-wheel model or bicycle model of a vehicle in longitudinal braking motion. This model captures the fundamental dynamic characteristics of the system in a simple form and it is widely used by control engineers and researchers. The dynamic equations are given as,

$$\dot{v} = \frac{1}{m}(F_{xf} + F_{xr}) - C_r mg - \frac{D_a v^2}{m} + g\sin\theta \quad (2)$$

$$\dot{\omega_f} = \frac{1}{I_\omega}(-F_{xf} r + T_{bf}) \quad (3)$$

$$\dot{\omega_r} = \frac{1}{I_\omega}(-F_{xr} r + T_{br}) \quad (4)$$

$$F_{zf} = \frac{m}{2(l_f + l_r)}(g l_f - h a_x) \quad (5)$$

$$F_{zr} = \frac{m}{2(l_f + l_r)}(g l_r + h a_x) \quad (6)$$

$$F_{x_f} = F_{z_f} \mu(\lambda_f, \lambda_r) \quad (7)$$

$$F_{x_r} = F_{z_r} \mu(\lambda_r, \lambda_f) \quad (8)$$

where the rolling resistance $C_r\, mg$, wind drag force $D_a\, v^2$ and road gradient $g\, \sin\theta$ are considered. T_{bf} and T_{br} are the braking torques applied to the front and rear wheels respectively. F_{xf} and F_{xr} are the front and rear longitudinal tyre forces. F_{zf} and F_{zr} are the vertical tyre forces at the front and rear wheels. ω_f and ω_r are the angular velocities of the front and rear wheels respectively and a_x is the acceleration of the vehicle. The vehicle mass is denoted m, I_ω is the moment of inertia of the wheel and r is the wheel radius. l_f and l_r are the distances from the vehicle centre of gravity to the front and rear axle and h is

the height of the Centre of Gravity (COG), μ is the tyre-road friction coefficient and λ is the relative wheel slip which is given as follows

$$\lambda_f = \frac{v-\omega_f r}{v} \tag{9}$$

$$\lambda_r = \frac{v-\omega_r r}{v} \tag{10}$$

where λ_f, λ_r are the front and rear wheel slips respectively. Hence, the slip dynamic equations can be derived as follows assuming the road gradient is negligible.

$$\dot{\lambda}_f = \frac{-1}{v}\left(\frac{1-\lambda_f}{m} + \frac{r^2}{J}\right) F_{Z_f}\mu(\lambda_f, \lambda_r) + \frac{r}{vJ}T_{bf} \tag{11}$$

$$\dot{\lambda}_r = \frac{-1}{v}\left(\frac{1-\lambda_r}{m} + \frac{r^2}{J}\right) F_{Z_r}\mu(\lambda_r, \lambda_f) + \frac{r}{vJ}T_{br} \tag{12}$$

2.3 Hydraulics and Electro Mechanical Brake (EMB) system.

The hydraulic or pneumatic brake system is modelled as a first order system as in Guo et al (2014). The hydraulic brake torque T_{bhy} is proportional to the cylinder pressure P

$$T_{bhy} = k_b P \tag{13}$$

where $k_b > 0$

$$P_r = \tau\dot{P} + P \tag{14}$$

P_r is the pressure inside the reservoir and τ is the time constant of the pipelines. The atmospheric pressure is assumed small and neglected.

The EMB model consists of an electric motor, a gearing device and brake pads. The electric braking torque T_{bm} of the electric motor is given as

$$T_{bm} = K_e \Omega \tag{15}$$

where K_e is the electromotive force coefficient and Ω is the rotational speed of the motor. Here, it is assumed that the motor torque is proportional to motor rpm which is a function of vehicle speed in regenerative mode.

The power demanded via the brake control subsystem reaches the battery pack. If the demanded power is positive the battery is discharged and charged when the demanded power is negative. The battery continuous power limit represents the prior known power limit of the battery given the manufacturer data available. Given that, in general, Lithium-ion cells can withstand a peak power (short duration) that is significantly higher than its continuous power rating it was necessary to carry out cell testing to estimate the battery peak power limit.

$$P_{batt} = \eta P_{act} \tag{16}$$

$$I_{batt} = \frac{P_{batt}}{V_{batt}} \tag{17}$$

where P_{batt} and P_{act} are the power of battery and power actual respectively, η is the electric motor-generator efficiency, I_{batt} is the current that recharges the battery and V_{batt} is the total voltage of the battery pack. The battery current limit determines the recharge and discharge limit of the battery pack and it is estimated for a particularly severe deceleration profile in the next section with corresponding brake force distribution.

3. BRAKE FORCE DISTRIBUTION

Equations (5) and (6) give the normal forces acting on the front and rear wheels during deceleration considering the static weight distribution of the car and the dynamic mass transfer. To maintain stability during severe acceleration and ensure maximum energy recuperation, t to keep the maximum friction on the rear wheel higher than on the front wheel.

$$\mu_{max} < \left(\frac{F_x}{F_z}\right)_r \leq \left(\frac{F_x}{F_z}\right)_f < 0 \tag{18}$$

Hence, the brake force distribution is given in Fig. 3. A front deceleration force distribution of 60% was selected.

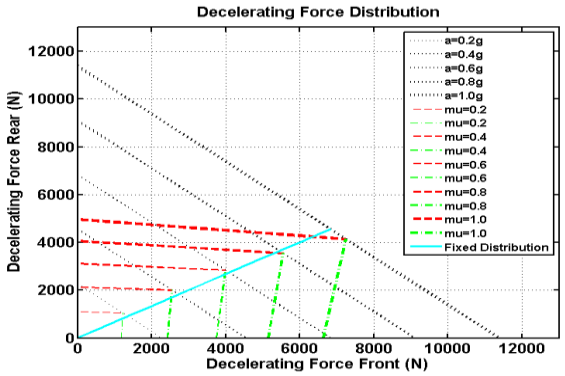

Fig.3. Brake force distribution

At the highest deceleration (1g) the friction limit of the rear axle is exceeded to meet requirement (18). This will define the maximum force the rear axle is required to produce. The graph of adhesion utilisation against rate of braking (deceleration/g) in Fig. 4 shows that the rear axle will lock for a friction coefficient $\mu > 0.7$. Fig. 5 shows that the power of the electric machines is sufficient to achieve a 1g stop from 100 km/h, based on a rear brake distribution of no more than 40%. The battery continuous power limit represents the prior known power limit of the battery given the manufacturer data available. This is approximately 25% of the power required by the rear axle at 100 km/h. A hybrid distribution between the ideal curve and the United Nations Economic Commission for Europe (UN/ECE13) regulation curve for an EV is generated based on the demand and battery limits.

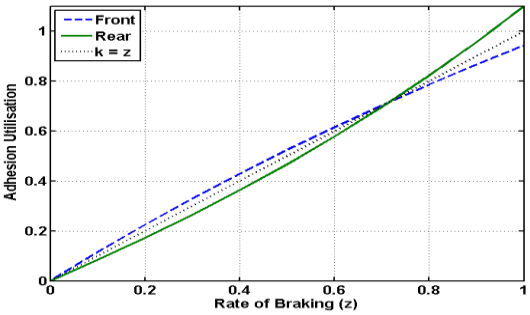

Fig.4. Adhesion utilization against rate of braking

The powertrain, including the electric machines and the battery pack, should be capable of absorbing 126kW peak power. The electric machines in the Delta E4 Coupe meet this requirement. To calculate the battery current, it has been assumed that the battery voltage remains at its nominal voltage, 317 V.

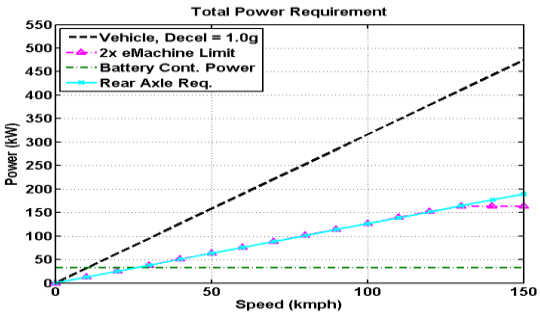

Fig.5.Total power requirement

This is valid since during charging, the battery pack's voltage will be increased, meaning that the battery voltage is likely to be above its nominal voltage for the majority of its operating range of State of Charge (SoC) so this estimate is likely to be a critical value.

The resulting battery current profile for the Delta E4 Coupe decelerating at 1g from 100 km/h is shown in Fig.6. The estimated peak battery current is 399A.

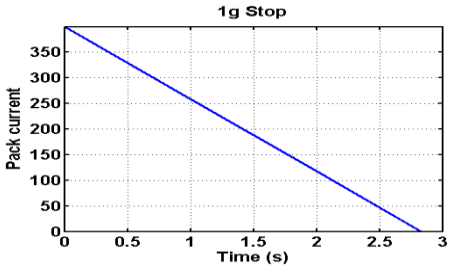

Fig.6. Theoretical battery pack current profile for 1g stop from 100kph

4. OPTIMAL SLIP GENERATION AND BRAKE TORQUE LIMITER

4.1 Optimal slip generation

The required maximum brake force to achieve maximum braking efficiency in order to stop the vehicle as quickly as possible without locking the wheels and losing steerability is a function of the maximum frictional coefficient of the road. In reality, optimal slip varies continuously with changing road conditions. The Magic Formula (MF) or Pacejka model (H. B. Pacejka et al, 2002) is used to describe the tyre-road interaction. It is a widely used tyre model to calculate the steady-state tyre forces and moments. It is a semi-empirical model and is given as follows

$$y(x) = D\sin[C\arctan Bx - E(Bx - \arctan Bx)] \quad (19)$$

where B = Stiffness factor, C = Shape factor, D = Peak value, E = Curvature factor.

The maximum braking force will be generated at the optimal slip λ_d. Therefore, one can find,

$$\frac{dy}{dx}\Big|_{(x=\lambda_d)} = 0 \quad (20)$$

From the Magic formula, it follows that

$$\frac{dy}{dx} = \frac{BCD}{(1+[Bx(1-E)+E\arctan(Bx)]^2)} [1 - E + \frac{E}{(1+B^2x^2)}]\cos C\arctan[Bx(1-E) + E\arctan(Bx)] \quad (21)$$

Equations (20) and (21) yield

$$\cos C\arctan[B\lambda^d(1-E) + E\arctan(B\lambda)] = 0 \quad (22)$$

Therefore, the optimized slip can be expressed as

$$\lambda_d = \frac{\tan(0.5)\pi/C - E\arctan(B\lambda)}{B(1-E)} \quad (23)$$

The shape coefficients *B, C, D, E* of the Magic formula are updated using an Extended Kalman Filter (EKF) based on tyre data as described in Rajendran et al (2017).

4.2 Supervisory brake torque limiter

A supervisory logic-based regulator or limiter is designed to monitor the distribution pattern described in section 3.

$$\begin{aligned} &If SOC > 75\% Then T_{br} = 40\% \\ &If SOC < 75\% \text{ and } T_{br} < maxT_{bm}\ Then\ T_{br} > 40\% \\ &If SOC > 75\% \text{ and } T_{br} < maxT_{m}\ Then\ T_{br} < 40\% \end{aligned} \quad (24)$$

The logic is adapted to maintain the rear wheel force distribution of 60% and SOC of 75%. The logic block regulates the torque demanded by the slip controller which is discussed in the next section. This not only regulates the hybrid torque distribution pattern addressed in section 4, but also protects the battery from overcharging considering SOC limits.

5. SLIDING MODE CONTROL

5.1 Controller design

A SMC controller is designed considering the actuator dynamics to track the optimal slips of the front and rear wheels. First, the sliding surfaces for the front and rear wheels are defined and then the desired brake torques are derived. The hydraulic and electric torques given in (13) and (15) are substituted in (11) and (12) to obtain the new slip dynamics of the front and rear wheels as described below.

$$\dot{\lambda}_f = \frac{-1}{v}(\frac{1-\lambda_f}{m} + \frac{r^2}{J})F_{Z_f}\mu(\lambda_f, \lambda_f) + \frac{r}{vJ}T_{bhy} \quad (25)$$

$$\dot{\lambda}_r = \frac{-1}{v}(\frac{1-\lambda_r}{m} + \frac{r^2}{J})F_{Z_r}\mu(\lambda_r, \lambda_f) + \frac{r}{vJ}T_{bm} \quad (26)$$

The sliding surfaces of the front and rear wheels are chosen as follows

$$s_i = \lambda_i - \lambda_{di} \quad (27)$$

where $i = f, r$ (front and rear wheels respectively).

λ_{di} is the slip ratio that provides maximum friction force and the error equation of slip ratio is defined as $e_i = \lambda_i - \lambda_{di}$, so the controller should try to minimize this error. The sliding motion occurs when the states reach the sliding surfaces defined by $s_i = 0$. The control effort required, on average, to maintain the states on the sliding surface is termed the equivalent control and here it is name, equivalent brake torque, T_{eqi}. The dynamics in the sliding motion satisfy

$$\dot{s_\iota} = 0 = \dot{\lambda_\iota} - \dot{\lambda_{d\iota}} \tag{28}$$

Then by substituting (25) and (26) in (28) one can obtain

$$0 = \frac{1}{v}\left[\frac{-r}{J}(F_{xi}r - T_{bi}) + (1-\lambda_i)\dot{v}\right] - \dot{\lambda}_{di} \tag{29}$$

Then the equivalent brake control torque, T_{eqi}, is obtained assuming the desired slip is constant as follows

$$T_{eqi} = F_{xi}r - (1-\lambda_i)\frac{\dot{v}J}{r} \tag{30}$$

An additional control torque T_{bhi} is required to force the states to stay on the sliding surface or to reject any disturbance. T_{bhi} is determined by the following reaching condition

$$s_i\dot{s_\iota} < -\eta_{si}\left|s_i\right| \tag{31}$$

where η is a strictly positive design parameter. Using (25) and (26), (28) can be rewritten as

$$s_i\dot{\lambda_\iota} < -\eta_s\left|s_i\right| \tag{32}$$

Substitution of (25) and (26) into (29) results in

$$\frac{s_i}{v}\left(\frac{-r}{J}\left(F_{xi}r - \left(T_{beqi} - T_{bhi}sgn(s)\right)\right) + (1-\lambda_i)\dot{v}\right) < -\eta_{si}\left|s_i\right| \tag{33}$$

Solving (33) to obtain T_{bhi} results in

$$T_{bhi} = \frac{vJ}{r}(F + \eta_{si}) \tag{34}$$

where $F \geq ((1-\lambda)\left|\dot{v} - \hat{\dot{v}}\right|)$ and $\hat{\dot{v}}$ is the estimate of the vehicle longitudinal acceleration. This is estimated by an EKF. The overall torque T_{bi} can be described as

$$T_{bi} = T_{beqi} - T_{bhi}sgn(s) \tag{35}$$

To eliminate the chattering problem the discontinuous switching function is replaced by the continuous function given by

$$f(s) = \frac{s}{|s|+\delta} \tag{36}$$

where $\delta > 0$. Therefore, the total brake torque T_{bi} is given by

$$T_{bi} = F_{xi}r - (1-\lambda_i)\frac{\hat{\dot{v}}J}{r} - \frac{vJ}{r}(F+\eta_s)f(s) \tag{37}$$

5.2 Simulation test results

An extreme braking scenario of decelerating from 30m/s or 100km/h at 1g m/s^{-2} is simulated to validate the proposed intelligent sliding mode scheme. Considering the adhesion utilization illustrated in Fig.4 braking is performed on a road of frictional coefficient 0.7. A hybrid torque distribution is generated considering the coupling between the front and rear slips. It is important to note that there are no friction brakes on rear wheels in this unique configuration. The simulation tests are performed with a full car model of 14th order and the performance of the proposed scheme is compared with the FSMC presented by J. Guo et al (2014).

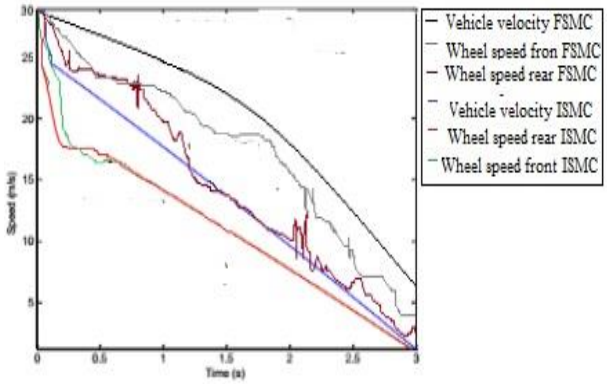

Fig.7. Vehicle velocity and wheel speed responses of proposed SMC and FSMC by Guo et al (2014).

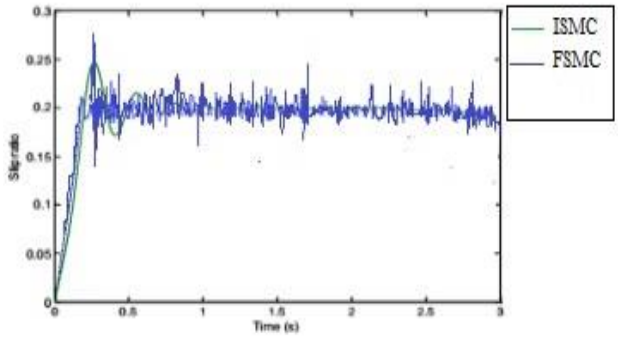

Fig.8. Comparison of slip tracking by proposed SMC and FSMC

The proposed ISMS produced a more rapid and smooth decrease in both vehicle velocity and wheel speed compared to the FSMC (Fig.7). It must be noted that the FMSC failed to produce the expected deceleration of 1g m/s^{-2} by exceeding the desired stopping time of 3s. It can be seen in Fig. 8 that the proposed SMC produced a much better slip response than the FSMC. The slip response of the FSMC is very oscillatory compared to the one produced the by proposed ISMS.

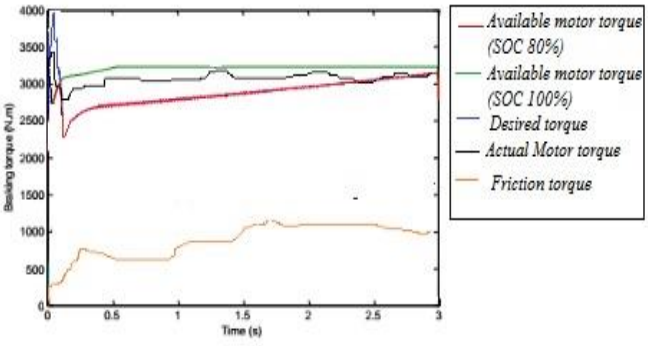

Fig.9. Distribution of Braking Torques

Regarding motor torque regulation, there is an initial spike in motor torque beyond the maximum limit. However, appropriate distribution of torque is executed quickly, and the generated motor torque is kept below its limit thereafter but close enough to produce maximum recuperation efficiency.

6. CONCLUSIONS

The Intelligent Sliding Mode Scheme (ISMS) presented, which has a simple logic-based torque limiter, produced good tracking of desired slip during a severe braking scenario with high braking efficiency. Moreover, it successfully maintained considerable energy recuperation without overcharging the battery pack by effectively following the chosen brake torque distribution pattern. Furthermore, it exhibited better results than a notable FSMC controller found in the HEV literature. Though the scheme is tested with a high-fidelity model in the Matlab/Simulink platform, experimental validation is required. In the future, Higher Order SMC (HOSMC) will be explored with Fuzzy Logic or ANN to generate an HEV system to improve overall performance.

REFERENCES

Bera, T., Bhattacharyya, K., Samantaray, K. (2011) Bond graph model-based evaluation of a sliding mode controller for combined regenerative and antilock braking system, *Proceedings of the Institution of Mechanical Engineers, Part I: Journal of Systems and Control Engineering,* Vol. 225, No. 7, pp. 918-934.

Guo, J., Jian, X., and Lin, G. (2014) Performance Evaluation of an Anti-Lock Braking System for Electric Vehicles with a Fuzzy Sliding Mode Controller", *Energies,* Vol. 7, No. 10, pp. 6459-6476.

Hamzah, N., Sam, M.Y., and Basari, A.A. (2007) Enhancement of driving safety feature via sliding mode control approach, *Fourth International Conference on Computational Intelligence, Robotics and Autonomous Systems*, pp. 116-120.

Jianjun, H., Zihan, G., Hang, P., and Dawei, Z. (2017) Research on regenerative braking control strategy of plug-in hybrid electric vehicle considering CVT ratio rate of change, *Proceedings of the Institution of Mechanical Engineers, Part D: Journal of Automobile Engineering*, https://doi.org/10.1177/0954407017735681.

Jing, Y., Mao, Y., Dimirovski, G. M., Zheng, Y., and Zhang, S. (2009) Adaptive global sliding mode control strategy for the vehicle antilock braking systems, *American Control Conference*, pp. 769-773.

Kayacan, E., Oniz, Y., and Kaynak, O. (2009) A grey system modeling approach for sliding-mode control of antilock braking systems, *IEEE Transactions on Industrial Electronics*, Vol.56, No.8, pp. 3244-3252.

Oniz, Y., Kayacan, E., and Kaynak, O. (2007) Simulated and experimental study of antilock braking system using grey sliding mode control, *IEEE International Conference on Systems, Man and Cybernetics*, pp. 90-95.

Pacejka, H. B. (2002) *Tyre and Vehicle Dynamics*, 3rd ed. Butterworth-Heinemann ch. 4.

Park, E.J., Stoikov, D., Falcao da Luz, L., and Suleman, A. (2006) A performance evaluation of an automotive magnetorheological brake design with a sliding mode controller, *Mechatronics*, Vol. 16, No. 7, pp. 405-416.

S. Rajendran, S. Spurgeon, G. Tsampardoukas and R. Hampson (2017) "Time-varying sliding mode control for Electric Car (EC)" *20th IFAC World Congress,* Toulouse, France, Vol. 50, issue 1, Pages 8490-8495.

Song, J. (2005) Performance evaluation of a hybrid electric brake system with a sliding mode controller, *Mechatronics*, Vol. 15, No. 3, pp. 339-358.

Tur, O., Ustun, O., and Tuncay, R.N. (2007) An introduction to regenerative braking of electric vehicles as anti-lock braking system, *Proceedings of the 2007 IEEE Intelligent Vehicles Symposium, Istanbul, Turkey*, pp. 944–948.

Unsal, C., and Kachroo, P. (1999) Sliding mode measurement feedback control for antilock braking systems, *IEEE Transactions on Control Systems Technology*, Vol. 7, No. 2, pp. 271-281.

Wu, M., and Shih, M. (2001) Simulated and experimental study of hydraulic anti-lock braking system using sliding-mode PWM control, *Mechatronics,* Vol. 13, No. 4, pp. 331-351.